

# Thin Film III-V Devices Integrated on Silicon-On-Insulator Waveguide Circuits

G. Roelkens, J. Brouckaert, D. Van Thourhout, R. Baets

Department of Information Technology, Ghent University, Ghent, Belgium

Thin film InP/InGaAsP active opto-electronic devices were fabricated on top of Silicon-on-Insulator waveguide circuits. Device integration was done using adhesive die to wafer bonding. Both photodetectors and laser diodes were fabricated on and coupled to Silicon-on-Insulator waveguide circuits. Integration of laser diodes and photodetectors was done simultaneously using identical processing steps.

## Introduction

The integration of optical functionalities on chip has been a long standing goal. Integration of more functions onto a single chip has the benefit of the economy of scale, an increase in performance and reliability. Silicon-on-Insulator (SOI) is an attractive material system to fabricate large scale integrated waveguide circuits due to the large refractive index contrast. Moreover, these waveguide structures can be fabricated using standard CMOS processes, thereby increasing yield and reproducibility (1). For particular photonic functions like light amplification and electrically pumped lasers at telecom wavelengths, the InP/InGaAsP material system remains the material of choice, despite significant research in Silicon based active opto-electronic devices. For detection of light at telecom wavelengths, both InP/InGaAsP (2) and Germanium (3) are being envisaged for integration on a Silicon platform. Therefore, in this paper we will focus on the integration of InP/InGaAsP laser diodes and photodetectors on top of an SOI waveguide circuit.

## Die to wafer bonding of III-V layers on SOI waveguide circuits using DVS-bis-BCB

The integration of InP/InGaAsP epitaxial layer structures was done using an adhesive die to wafer bonding process described in (4). For this, DVS-bis-BCB is used as an adhesive due to its excellent planarization properties, its low shrinkage upon cure and the fact that no by-products are created during curing. The processing sequence is outlined in figure 1. The processed SOI waveguide wafer is spin coated with DVS-bis-BCB and the unprocessed InP/InGaAsP dies (from a few mm<sup>2</sup> to a few cm<sup>2</sup>) are bonded epitaxial layers down to the SOI waveguide wafer. After bonding the InP substrate is removed using a combination of mechanical grinding and wet chemical etching until an InGaAs etch stop layer is reached. This leaves the InP/InGaAsP epitaxial layer structure bonded to the SOI waveguide circuit. After bonding and substrate removal, the III-V components can be fabricated on a wafer scale and lithographically aligned to the underlying SOI circuit.

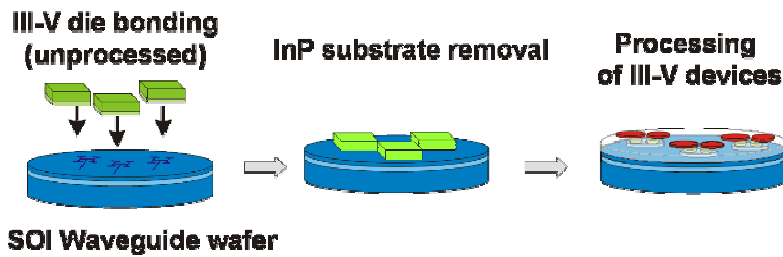


Figure 1. Heterogeneous integration of InP/InGaAsP on top of an SOI waveguide wafer by a die to wafer bonding process

### Integration of III-V photodetectors and laser diodes on SOI waveguide circuits

To demonstrate the versatility of the die to wafer bonding process, 3 types of InP/InGaAsP photodetectors and a Fabry-Perot laser diode were integrated on and coupled to an SOI waveguide circuit.

The first type of photodetector, a surface illuminated p-i-n photodetector is depicted in figure 2 together with a picture of the fabricated structures before top contact definition. Light from an SOI waveguide is coupled to the photodetector using a second order diffraction grating. This approach leads to small footprint components (the fabricated structures are  $10\mu\text{m}\times 10\mu\text{m}$ ) and allows for a thick DVS-bis-BCB bonding layer, which simplifies the bonding procedure. Responsivity is limited however, due to the loss of light towards the Silicon substrate, as the grating diffracts both upwards and downwards. This type of photodetector allows for a large optical bandwidth as is shown in the simulation in figure 3. Here the absorbed power fraction and reflected power back into the SOI waveguide is plotted as a function of the wavelength for a p-i-n photodetector consisting of a  $2\mu\text{m}$  thick InGaAs absorption layer and for  $2\mu\text{m}$  wide and  $50\mu\text{m}$  long detectors and gratings. The grating period is  $610\text{nm}$ , the etch depth of the grating is  $50\text{nm}$  and the duty cycle is 50%. The SOI waveguide core is  $220\text{nm}$  high.

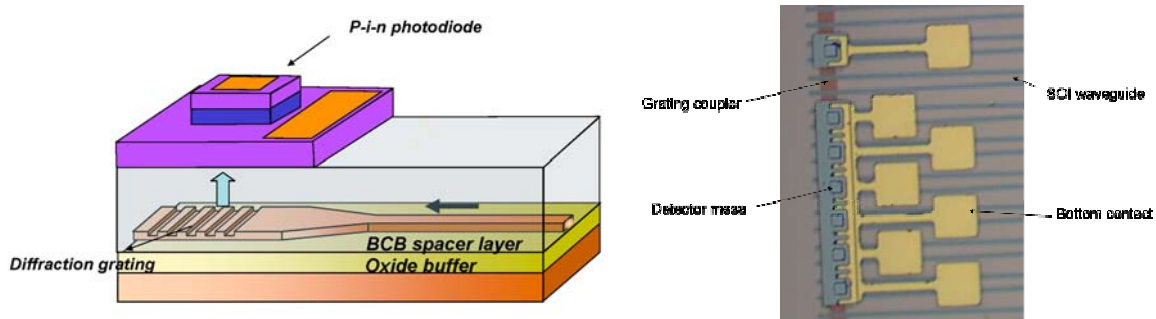


Figure 1. Coupling structure of a bonded surface illuminated photodetector and a top view picture of fabricated structures

In order to be able to integrate laser diodes and photodetectors at the same time in the same epilayer structure, the optimal detector layer stack containing a thick InGaAs absorption layer needed to be replaced by an active InGaAsP quantum well layer stack emitting at  $1550\text{nm}$ . Therefore the absorption was reduced due to the lower absorption layer thickness and lower absorption coefficient compared to the InGaAs case. Experimentally, a responsivity of  $0.02\text{A/W}$  was measured. This implies that integration of these types of photodetector together with laser diodes implies intrinsically a low

responsivity photodetector due to the boundary conditions of the laser layer structure. The integration of these types of photodetectors with functional SOI waveguide circuitry was shown in (2).

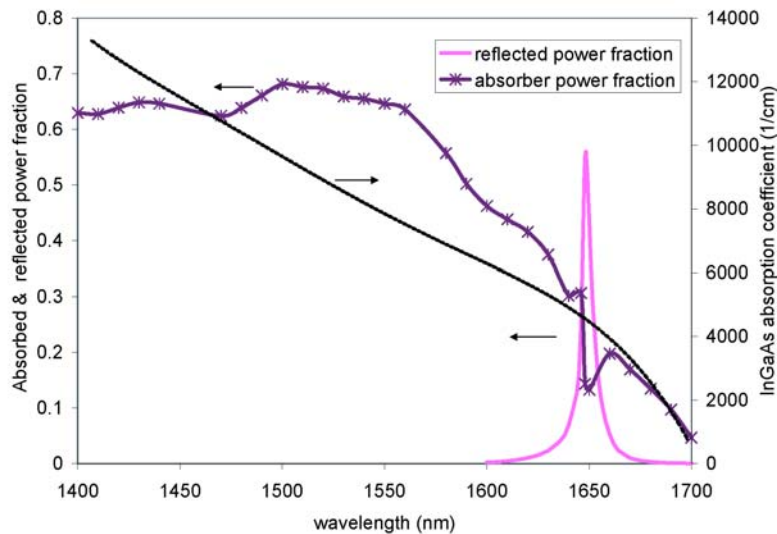


Figure 3. Simulation of the absorbed and reflected power fraction versus wavelength

An additional drawback of this type of photodetector is the large amount of processing steps required to fabricate the device. A second type of photodetector that was investigated is a metal-semiconductor-metal photodetector, as it is more easily fabricated, which is shown in figure 4. The layer structure consists of an undoped InGaAs absorption layer (205nm) and an InAlAs Schottky barrier enhancement layer (40nm). Light is coupled from the SOI waveguide to the photodetector by means of a directional coupler structure.

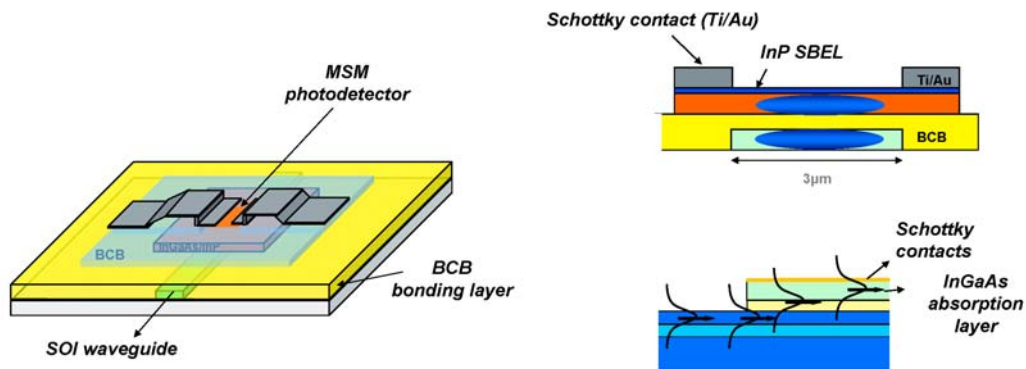


Figure 4. Metal-Semiconductor-Metal photodetector coupling structure

A top view of a fabricated MSM type photodetector is shown in figure 5, together with an IV-characteristic of a device under illumination and without illumination. A responsivity of 0.08A/W was obtained for a first batch of devices. The optical bandwidth is larger than 100nm and device footprint is small (fabricated devices were 3µm wide and

20 $\mu\text{m}$  long). Although easy to fabricate, the layer structure does not lend itself to integrate laser diodes and photodetectors in the same layer structure.

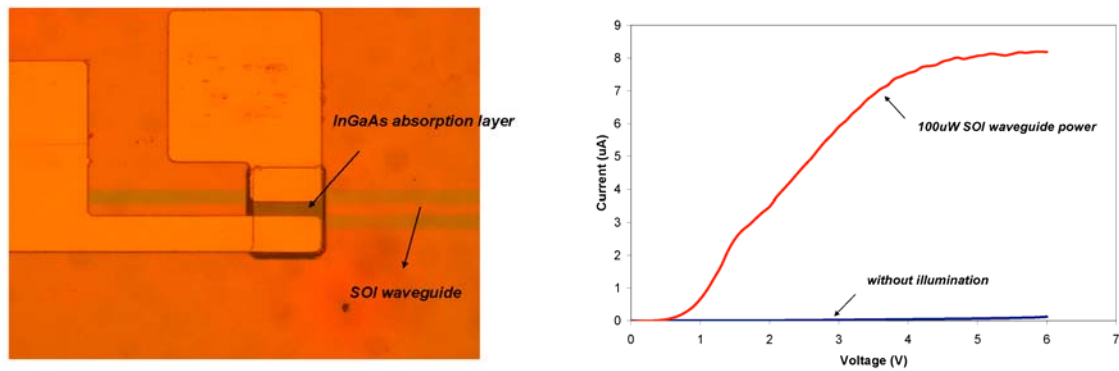


Figure 5. Fabricated devices and measured current versus voltage characteristic with and without illumination.

Therefore, a third type of photodetector was fabricated for which the integration of laser diodes can be done without compromising the responsivity of the photodetector. The coupling structure is depicted in figure 6. The coupling of light from the SOI waveguide to the InP/InGaAsP photodetector is done using an inverted taper approach to couple light into a polymer waveguide on top of the SOI, which is then butt coupled to the InP/InGaAsP active device as shown in figure 6. A top view of a fabricated structure is also shown. The inverted taper approach has been shown to be a large optical bandwidth (over 300nm optical bandwidth was shown) and high efficiency coupling structure. Theoretically, the coupling loss at the polymer/III-V interface is about 1.5dB. The polymer waveguide is a 1.3  $\mu\text{m}$  high polyimide waveguide ( $n=1.67$ ) and is 3 $\mu\text{m}$  wide. The SOI waveguide tapers from a 590nm wide single mode waveguide to an SOI taper tip of 175nm thereby adiabatically transforming the SOI waveguide mode to the mode of the polymer waveguide. The layer stack of the III-V structure was designed for an optimal coupling between the fundamental III-V waveguide mode and the polymer waveguide mode. It consists of a 600nm n-type InP undercladding, six InGaAsP quantum wells with a bandgap wavelength of 1550nm in between two separate confinement layers of 150nm (bandgap wavelength 1.25 $\mu\text{m}$ ) and a 2 $\mu\text{m}$  p-type InP and 150nm p++ InGaAs contact layer. A device responsivity of 0.23A/W was measured.

The same layer structure, coupling scheme and processing sequence can be used to fabricate bonded laser diodes. Laser emission and coupling of light to an SOI waveguide was observed as shown in figure 7. The threshold current density is large however (10.4kA/cm<sup>2</sup> for a 500 $\mu\text{m}$  long device) and only pulsed operation was obtained. The large threshold current density is related to the quality of the etched laser facets. No CW operation was obtained due to the large thermal resistance of the device, caused by the low thermal conductivity of the DVS-bis-BCB bonding layer. This can however be circumvented by mounting the device structure p-side down on a heat sink or by incorporating a heat sink structure close to the laser diode as in (5).

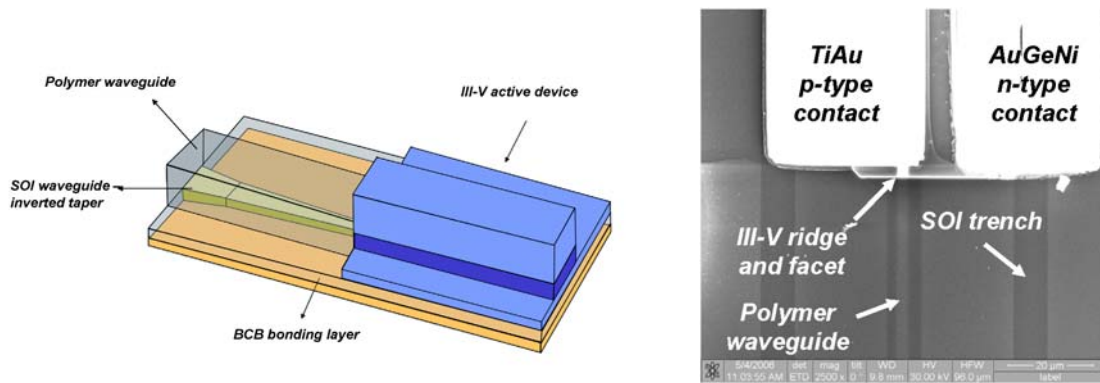


Figure 6. Bonded photodetector structure based on an inverted taper structure. Top view of fabricated structure. The inverted SOI taper is not visible as it is buried underneath the polymer waveguide.

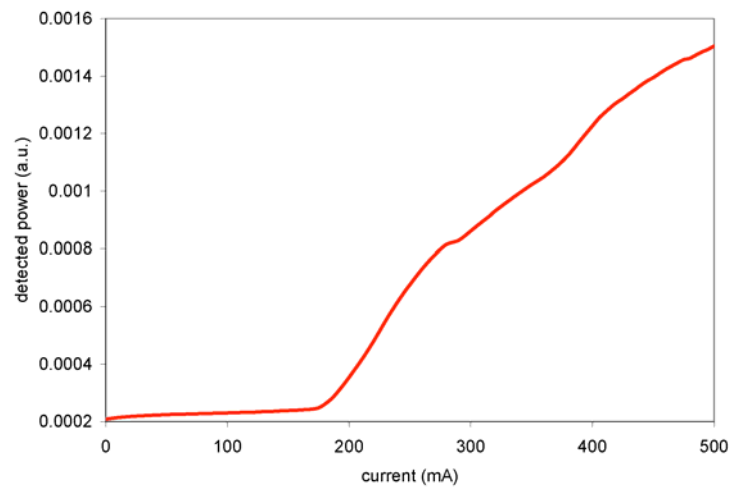


Figure 7. Power – current characteristic of the bonded laser diode. Light is collected from the SOI waveguide using a lensed fiber.

## Conclusions

We designed and fabricated three types of InP/InGaAsP photodetectors on Silicon-on-Insulator waveguide circuits. Each type of photodetector has its own advantages and drawbacks. The simultaneous integration of photodetectors and laser diodes was demonstrated, which opens the way for low cost optical integrated circuits for telecommunication applications.

## Acknowledgements

This work was partly supported by the European union through the Network of Excellence ePIXnet and the IST PICMOS project, by the Belgian IAP-PHOTON network the IWT-GBOU project and the Fund for Scientific Research (FWO). The authors would like to thank Meint Smit for the fruitful discussions.

## References

1. W. Bogaerts, R. Baets, P. Dumon, V. Wiaux, S. Beckx, D. Taillaert, B. Luyssaert, J. Van Canpenhout, P. Bienstman and D. Van Thourhout, *Journal of Lightwave Technology*, **23**, 401 (2005).
2. G. Roelkens, J. Brouckaert, D. Van Thourhout, R. Naets, R. Notzel and M. Smit, *Optics Express*, **13**, 10102 (2005)
3. L. Colace, G. Masini and G. Assanto, *Journal of Quantum Electronics*, **35**, 1843 (1999)
4. G. Roelkens, J. Brouckaert, D. Van Thourhout and R. Baets, *210<sup>th</sup> ECS Meeting* (2007)
5. I. Christiaens, G. Roelkens, K. De Mesel, D. Van Thourhout and R. Baets, *Journal of Lightwave Technology*, **23**, 517 (2005)